KSME

Springer

Journal of Mechanical Science and Technology 38 (8) 2024

Original Article
DOI 10.1007/s12206-024-0713-9

Keywords:
· CFD
· Gerotor pump
· Noise reduction
· Port shape
· Pressure oscillations
· Vibrations
· Noise reduction

Correspondence to:
Chang Hyun Sohn
chsohn@knu.ac.kr

Citation:
Nazir, K., Sohn, C. H. (2024). Reduction of delivery pressure fluctuations in a gerotor pump. Journal of Mechanical Science and Technology 38 (8) (2024) 4161~4166.
http://doi.org/10.1007/s12206-024-0713-9

Received September 18th, 2023
Revised March 18th, 2024
Accepted April 7th, 2024

† Recommended by Editor
Han Seo Ko

Reduction of delivery pressure fluctuations in a gerotor pump

Kamran Nazir[1] and Chang Hyun Sohn[2]

[1]Department of Mechanical Engineering, National University of Technology (NUTECH), Islamabad 44000, Pakistan, [2]School of Mechanical Engineering, Kyungpook National University, Daegu 702-701, Korea

Abstract Generated rotor (gerotor) pumps have commercial applications in oil supply pumps and compressors. Unfortunately, they produce an excessive amount of noise while in operation. The present study focuses on reducing the noise, which is caused due to pressure oscillations in the fluid, and vibration levels when a gerotor pump is in operation. Three-dimensional numerical simulations were performed on the gerotor pump using the dynamic mesh method. The flow field was simulated using the commercial software Ansys Fluent. The mesh motion was provided in the form of a user-defined function. Computational fluid dynamics analysis was performed for different combinations of delivery pipe length and diameter, and their effects on delivery pressure were analyzed. It is observed from numerical results that the pressure oscillations are reduced around 20 % by increasing volume of port or pipe region, which in turn reduces the noise levels. It is concluded that the pressure oscillations during the fluid flow are highly dependent on the volume of the delivery pipe.

1. Introduction

Generated rotor (gerotor) pumps have numerous applications, including lubrication and cooling of automobile engines. Their main advantage is their high flow rate and efficiency, but they produce excessive noise levels while in operation.

Numerous studies have focused on the design of rotor gears to improve the efficiency of gerotor pumps. Litvin and Feng [1] developed the epitrochoidal gearing surface using the differential geometry method. Demenego et al. [2] presented a computer program that determines the mesh motion in a single rotor revolution. This program also indicates errors caused due to the improper alignment of pump gears. Sasaki et al. [3] developed a new tooth profile for gerotor pumps named megafloid. They discovered that the theoretical volumetric flow rate can be increased by 10 % or more by utilizing a megafloid profile rather than parachoid profile. Yoshida [4] developed a novel tooth profile named geocloid, observing that the geocloid has a higher mechanical efficiency, resulting in smaller rotor size without decreasing the volumetric flow rate. Mimmi and Pennacchi [5] obtained transcendental equations for calculating the limit dimensions to avoid undercutting. Ye et al. [6] presented basic explicit formulas for calculating the limit dimensions to avoid undercutting in the inner rotor by examining the radius of curvature on the convex section. Hwang and Hsieh [7] presented a geometry design procedure for the hypotrochoidal gear pump (referred as “hypogerotor pump” in this paper) using the equidistant extended hypotrochoid curve, based on the theories of envelope and conjugate surfaces.

The visualization of fluid behavior within gerotor pumps poses a significant challenge, as direct inspection of the pump’s interior is hindered due to the housing and casing materials. Therefore, the prevalent approach involves the development of new prototypes and models using transparent materials. Itoh et al. [8] employed a unique coating to a large transparent gerotor pump model. They also employed light-reflecting tracer particles that resemble platelets, which enabled them to evaluate flow patterns and volumetric efficiency. Raush et al. [9] made significant advancements in experimental techniques for observing fluid flow characteristics. They introduced the time-resolved particle image velocimetry technique in a trochoidal gear

pump. Transparent methacrylate was used to manufacture the casing and outer gear, allowing for interior illumination of the trochoidal gear chambers. They utilized carefully selected alginate tracer particles known for their effective tracking and light-scattering properties, while also being gentle on the contact surfaces to avoid damage. The experimental results demonstrate good agreement with the numerical data.

In recent years, there has been a significant emphasis on computational fluid dynamics (CFD) tools to predict the key performance indicators in gerotor pumps. Hsieh et al. [10] performed a CFD analysis on multistage gerotor vacuum pumps using the dynamic meshing technique. They observed that the maximum efficiency in terms of flow parameters can be achieved using a parallel three-stage gerotor pump. Kwak and Kim [11] selected a gerotor design characterized by a higher flow rate compared to existing gerotor pumps. They optimized the port shape of the gerotor pump using CFD analysis, considering ten design parameters, with the primary goal of reducing irregularities. Based on the CFD analysis results, they developed an oil pump that incorporates the optimal gerotor design along with the newly improved port shape. This development successfully achieved a substantial reduction in irregularities while maintaining a high flow rate.

The gerotor pump system consists of a rotor, suction and delivery ports, and pipe sections. Kim et al. [12] performed an experimental and numerical study to analyze the effect of relief grooves at the surface of the port on pressure oscillations at the pump's outlet. They discovered that installing the relief grooves at the inlet port results in fluid leakage between the ports. In contrast, by installing the relief grooves on the outlet port not only reduces the pressure fluctuation but also provides better fluid delivery performance under different operational conditions. Abbas and Kumar [13] studied the two dimensional deformation in half space voids which are thermoelastic and are initially stressed. Marin et al. [14] proposed a new model which can be used to study the components of stress in fluid and solid phases particularly for porothermoelastic media. Kumar and Manonmani [15] performed CFD simulations on gerotor pumps to investigate the effects of various parameters such as fluid viscosity, number of ports, and rotor speed on the volumetric flow rate of the pump. The addition of ports on the cover plate has been demonstrated to result in an increase in flow rate and a decrease in pressure oscillation. Sung et al. [16] designed relief grooves on the port plate in order to reduce pressure fluctuations. They quantified the opening areas for configurations with and without relief grooves between the port plate and the chamber. They performed an experimental and numerical study to observe the effect of relief grooves on pressure fluctuations. The findings demonstrated that relief grooves proved highly effective in reducing and stabilizing pressure fluctuations both at the pump outlet and within the chamber.

The objective of this study was to reduce the gerotor pump's delivery pressure oscillations, which would result in decreased vibration and noise levels. In order to validate the current numerical model, the numerical results were compared with the published experimental data. The impact of outlet pipe volume variation on pressure oscillations was analyzed using the current numerical model. The pipe volume was varied by changing the length and diameter of the pipe.

2. Numerical methodology

The design parameters for the rotor of a gerotor pump are illustrated in Table. 1. ANSYS FLUENT 17 [17] was used to perform numerical simulations in current study. The domain is split into five zones: inlet pipe, inlet port, rotor, outlet pipe, and outlet port as illustrated in Fig. 1.

The mesh in each zone is generated individually and then connected. The interfaces developed at the top surface of rotor and bottom surface of port are merged together. The interface boundary condition is used at the newly generated surface so that the fluid flow can occur from rotor into port area.

Fig. 2 presents the grid independent study for rotor and port/pipe region of the gerotor pump. It is showing that when a small number of elements are being used either in rotor or port/pipe region, the calculated pressure is a small value. When the grid points are increased in both regions, the calculated pressure approaches a saturated value. Therefore, a final mesh size of approximately 650000 elements was selected for the pipe and port section and approximately 300000 elements for the rotor section. The grid in both the regions is of very quality with maximum aspect ratio of 5 in some regions.

In the current study, quadrilateral mesh elements were employed in rotor while triangular elements were used in port and pipe section of gerotor pump. The flow characteristics of a gerotor pump were modeled using unsteady simulations. For com-

Table 1. Design parameters of rotor.

Parameter	Value
Rotor gear profile	Megafluid
Inner gear teeth	7
Outer gear teeth	8
Rotational speed	2000 rpm
Mass flow rate	14.4 L/min

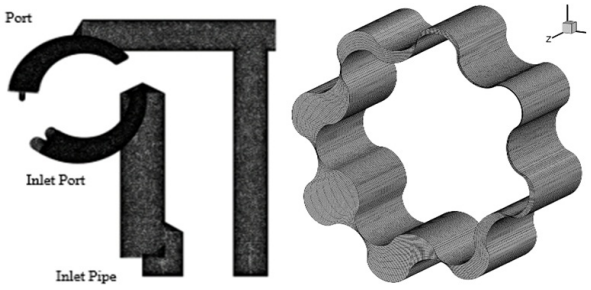

Fig. 1. Grid used in the current study: (a) port and pipe mesh; (b) rotor mesh.

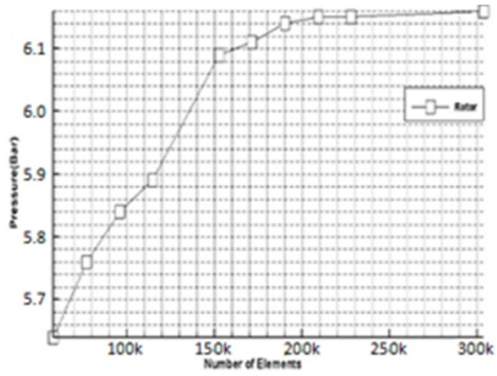

(a) Rotor case

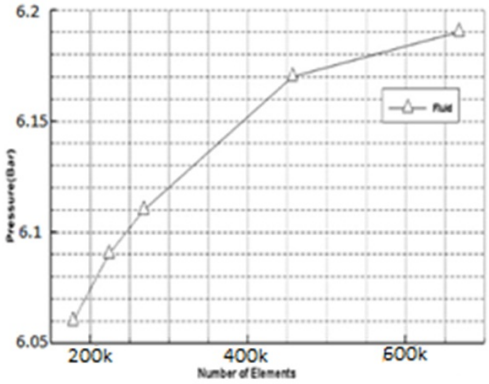

(b) Port and pipe case

Fig. 2. Results of the grid dependency calculation.

plete rotation of rotor (360 degree) with 2000 rpm, the required time (in seconds) was 2000/60, which will lead us to find time step required for one-degree rotation of rotor as follows,

$$time\,step = \frac{60}{2000 * 360}\,. \tag{1}$$

At the domain's inlet, 10 % of the turbulence intensity is initiated using the k-ε turbulence model. The PISO scheme is employed to accomplish pressure-velocity coupling. The least square cell-based scheme, PRESTO scheme, and first-order upwind scheme are employed to discretize the gradient, pressure, and momentum equations. A first-order implicit scheme is employed for temporal discretization. The pressure at inlet is taken as 0 bar, as the gerotor pump is providing lubricant from reservoir where the pressure is at atmospheric conditions. In current study, it is assumed that the pump will create the pressure difference of 6 bar and hence 6 bar pressure is applied at outlet. The smoothing and remeshing details of dynamic mesh are provided in the form of a user-defined function (UDF).

The general form of governing equation for a moving boundary can be expressed by Eq. (2),

$$\frac{d}{dt}\int \rho\phi dv + \int \rho\phi(\vec{u} - \overrightarrow{u_g})d\vec{A} = \int \Gamma \nabla\phi d\vec{A} + \int S_\phi dV \tag{2}$$

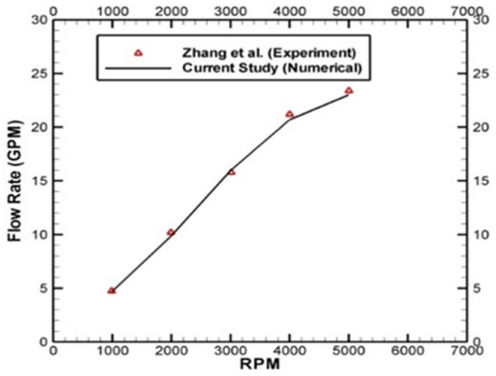

Fig. 3. Comparison of current numerical results with Zhang et al.'s experimental data.

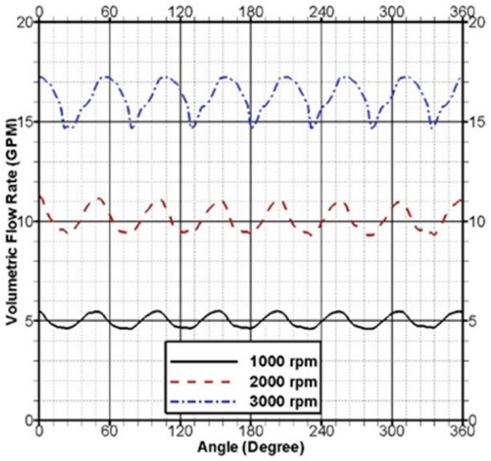

Fig. 4. Variation of flowrate with rotor speed for one cycle of rotation.

where ρ is the fluid density, $\vec{u}$ is the flow velocity vector, $\overrightarrow{u_g}$ is the grid velocity of the moving mesh, Γ is the diffusion coefficient, and S_ϕ is the source term of ϕ.

3. Results and discussion

Zhang et al. [18] conducted experimental and numerical study for gerotor pump speeds between 500 and 6000 rpm. They observed that the numerical results for the gerotor pump's discharge rate demonstrated good agreement with the experimental data. The numerical model employed in current study was used to simulate the zhang model and the results are compared.

The method used in current study is to develop two separate zones. One is the port and pipe region in which unstructured grid is employed. The second is the rotor zone in which a structured grid is used. The advantage of using this method is that it has much fewer grid points in the rotor region, which results in a decrease of computational cost without compromising results accuracy. As depicted in Fig. 3, the current numerical model also demonstrates good agreement with the experimental results of Zhang et al. Fig. 4 depicts the volumetric flow rate for

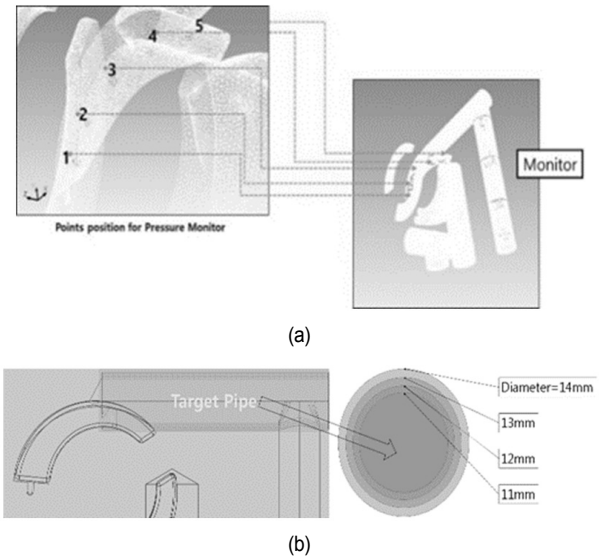

Fig. 5. Diameter variation and data collection points.

one complete rotation cycle of the gerotor at different pump speeds. It can be observed that the amplitude of the flowrate waves increases with increasing revolution speed. This can be because at higher revolutions, the flow rate is high, resulting in an increased dynamic pressure variation. In contrast, at low pump speeds (1000 rpm), the amplitude of flowrate is quite small due to the low flow rate of the gerotor pump.

The objective of this study is to analyze the effect of outlet pipe volume variation on the delivery pressure oscillation of the gerotor pump. The pipe volume is varied by changing the length and diameter of the outlet pipe. The pressure data is collected at several points in the delivery port and pipe as depicted in Fig. 5(a). Fig. 5(b) depicts the pipe diameter variations analyzed in the current study. The pipe diameter is increased from 11 mm to 14 mm, with 1 mm increment in each case.

Figs. 6(a) and (b) depict the distribution of instantaneous pressure in the port and pipe, respectively, for one complete rotation cycle of the rotor. It can be observed that as the diameter of the delivery pipe increases, the pressure oscillation decreases. The results of all diameter variation cases are summarized in Table 2. The average pressure in the port and pipe is approximately 6 bar, which is equal to the actual delivery pressure requirement. The maximum and minimum values in Table 2 correspond to the maximum and minimum pressure values during one complete rotation cycle of the rotor. The pressure fluctuation is the difference between the maximum and minimum pressure values during one complete cycle. It can be observed from Table 2 that by increasing the delivery pipe diameter from 11 mm to 14 mm, the pressure oscillation in the port area is reduced by approximately 22 % and in the outlet pipe region by approximately 16 %.

As depicted in Fig. 7, the length of the delivery pipe is increased by 20 %, and the effect of length increment on delivery pressure oscillation is observed. The pressure contours in the rotor and port and pipe sections are depicted in Fig. 9.

Table 2. Result summary for all diameter variation cases.

(Units: bar)		Average	Max	Min	Pressure fluctuation
1st model (11 mm)	Port	6.060	6.739	5.810	0.929
	Pipe	6.018	6.262	5.930	0.332
2nd model (12 mm)	Port	6.042	6.617	5.847	0.770
	Pipe	6.009	6.216	5.942	0.277
3rd model (13 mm)	Port	6.030	6.602	5.853	0.749
	Pipe	6.008	6.220	5.943	0.274
4th model (14 mm)	Port	6.028	6.573	5.858	0.715
	Pipe	6.009	6.218	5.945	0.273

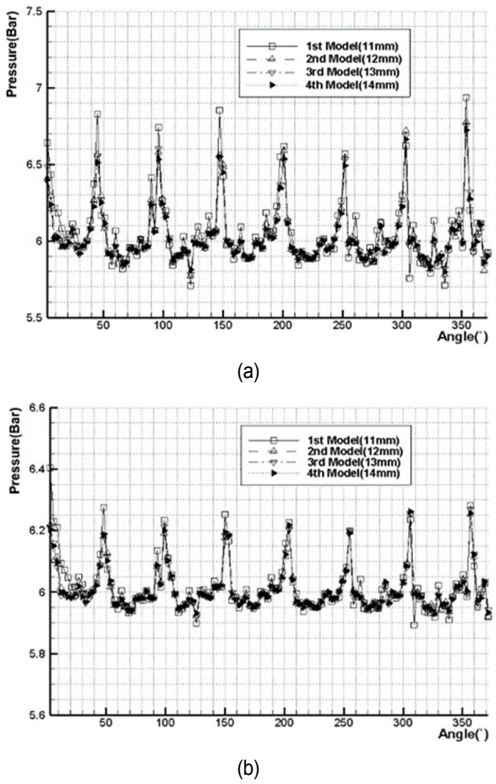

Fig. 6. Pressure oscillation for all diameter cases: (a) port; (b) pipe.

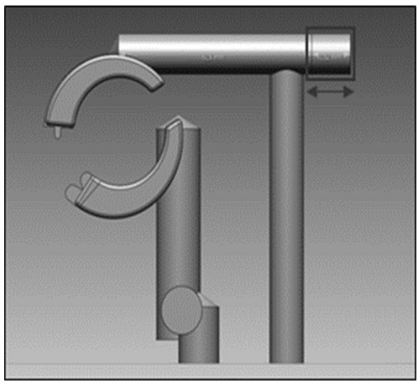

Fig. 7. Geometry of the gerotor pump with extended pipe length.

Table 3. Result summary for extended delivery pipe length cases.

(Units: bar)		Average	Max pressure	Min pressure	Pressure fluctuation
1st model	Port	6.060	6.739	5.810	0.929
	Pipe	6.020	6.262	5.930	0.332
2nd model	Port	6.043	6.647	5.856	0.791
	Pipe	6.009	6.212	5.946	0.266

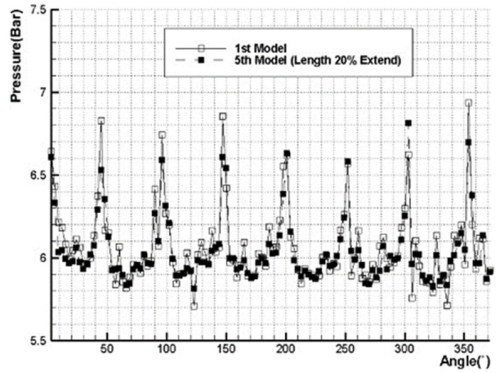

(a)

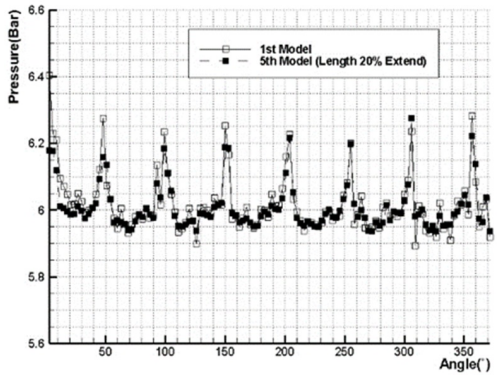

(b)

Fig. 8. Pressure contours: (a) rotor; (b) port and pipe.

The instantaneous pressure distribution for one complete rotation cycle of the rotor for both the original and extended length models is depicted in Fig. 8. It can be observed that the peak pressure values for the extended pipe are lower compared to the original model. The increased volume either in port or pipe region acts as a pressure release valve and hence results in a decrease in pressure fluctuation caused by rotor motion. This can be seen in the graphs of Fig. 8 that the pressure fluctuation for increased volume case is much less as compared to the original case.

Table 3 illustrates the average, maximum, and minimum pressure values for the extended and original pipe length cases. The average pressure in the port and pipe region is 6 bar. The pressure oscillation is reduced by 0.138 bar, which is approximately 15 % reduction in the port region, and by 0.066 bar, which is approximately 20 % reduction in pipe region.

Table 4. Result summary for extended delivery pipe length cases.

Design variation		Monitor	Pressure fluctuation (bar)	Change in pressure fluctuation (%)
Diameter	1st model	Port	0.929	-
		Pipe	0.332	-
	2nd model	Port	0.770	16 %
		Pipe	0.274	16 %
	3rd model	Port	0.749	18 %
		Pipe	0.277	15 %
	4th model	Port	0.715	22 %
		Pipe	0.273	16 %
Length	2nd model	Port	0.791	13 %
		Pipe	0.266	18 %

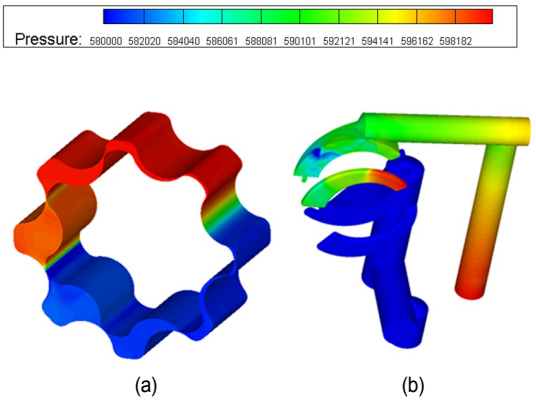

(a) (b)

Fig. 9. Comparison of pressure oscillations in extended pipe length cases: (a) port; (b) pipe.

Table 4 summarizes the results of pressure oscillation for all the cases investigated in this study. It is evident that increasing the pipe diameter to 14 mm is the most effective case for reducing pressure oscillation in the port region. In contrast, increasing the pipe length yields the best results for reducing pressure oscillation in the pipe region.

4. Conclusions

Gerotor pumps are internal-rotary, positive displacement pumps commonly employed for engine lubrication due to their high volumetric efficiency. During the operation of a gerotor pump, high pressure oscillations occur, resulting in high noise and vibration in the pump's components. The objective of the current study is was to reduce the pressure oscillations in the gerotor pump. In this study, the volume of the delivery pipe was increased by extending the length and diameter of the pipe. The effect of volume increment on pressure oscillations at the outlet port was analyzed. It is observed that increasing the pipe diameter reduces pressure oscillations in the outlet port by 22 %, while increasing the pipe length reduces pressure oscillations in the delivery pipe by 18 %.

Acknowledgments

This work was supported by the National Research Foundation of Korea (NRF) grant funded by the Korea government (MSIT) (2022R1F1A1061903).

Nomenclature

P : Pressure
rpm : Revolutions per minute

References

[1] F. L. Litvin and P.-H. Feng, Computerized design and generation of cycloidal gearings, *Mechanism and Machine Theory*, 31 (7) (1996) 891-911.
[2] A. Demenego, D. Vecchiato and F. L. Litvin, Nicola nervegna, and salvatore mancó, design and simulation of meshing of a cycloidal pump, *Mechanism and Machine Theory*, 37 (3) (2002) 311-332.
[3] H. Sasaki, N. Inui, Y. Shimada and D. Ogata, Development of high efficiency P/M internal gear pump rotor (megafloid rotor), *Sei. Technical Review-English Edition*, 66 (2008) 124.
[4] K. Yoshida, M. Uozumi, Y. Shimada and T. Kosuge, Development of high efficiency internal gear pump rotor geocloid rotor, *SEI. Tech. Rev.*, 74 (2012) 43-47.
[5] G. C. Mimmi and P. E. Pennacchi, Non-undercutting conditions in internal gears, *Mechanism and Machine Theory*, 35 (4) (2000) 477-490.
[6] Z. Ye, W. Zhang, Q. Huang and C. Chen, Simple explicit formulae for calculating limit dimensions to avoid undercutting in the rotor of a cycloid rotor pump, *Mechanism and Machine Theory*, 41 (4) (2006) 405-414.
[7] Y.-W. Hwang and C.-F. Hsieh, Geometric design using hypotrochoid and nonundercutting conditions for an internal cycloidal gear, *J. Mech. Des.*, 129 (4) (2007) 413-420.
[8] T. Itoh, Y. Murai, Y. Ueno, H. Oiwa, N. Miyagi and F. Yamamoto, Visualization of internal flow in an inscribed trochoid gear pump, *J. Vis. Soc. Jpn.*, 25 (2005) 303-304.
[9] G. Raush, P. J. Gamez-Montero, R. Castilla and E. Codina, Experimental study on the impulsion port of a trochoidal wheeled pump, *Flow Measurement and Instrumentation*, 55 (2017) 13-22.
[10] C.-F. Hsieh, T. Johar and Y.-T. Li, Flow characteristics of gerotor vacuum pumps with multistage designs, *Vacuum*, 196 (2022) 110787.
[11] H. Kwak and C. Kim, Design of port shape for reducing irregularity of oil pump, *J. of Mechanical Science and Technology*, 31 (2017) 5839-5848.
[12] S. Y. Kim, Y. J. Nam and M. K. Park, Design of port plate in gerotor pump for reduction of pressure pulsation, *J. of Mechanical Science and Technology*, 20 (10) (2006) 1626-1637.
[13] I. A. Abbas and R. Kumar, 2D deformation in initially stressed thermoelastic half-space with voids, *Steel Compos. Struct.*, 20 (5) (2016) 1103-1117.
[14] M. Marin, A. Hobiny and I. Abbas, The effects of fractional time derivatives in porothermoelastic materials using finite element method, *Mathematics*, 9 (14) (2021) 1606.
[15] M. S. Kumar and K. Manonmani, Numerical and experimental investigation of lubricating oil flow in a gerotor pump, *International J. of Automotive Technology*, 12 (6) (2011) 903-911.
[16] H.-J. Sung, H.-K. Min, Y.-J. Nam and M.-K. Park, Design and experimental verification of a port plate in a gerotor pump to reduce pressure pulsation, *J. of Mechanical Science and Technology*, 32 (2018) 671-678.
[17] Fluent Inc., *Fluent 17 Users Guide*, Fluent Inc., USA (2016).
[18] D. Zhang, C.-Y. Perng and M. Laverty, Gerotor oil pump performance and flow/pressure ripple study, *SAE Technical Paper* (2006) 2006-01-0359.

Kamran Nazir received his M.Sc. (Eng) in Mechanical Engineering from National University of Sciences & Technology, Pakistan. He received his Ph.D. in Mechanical Engineering from Kyungpook National University, South Korea. He works in the Mechanical Engineering Department at National University of Technology (NUTECH), Islamabad, Pakistan. His research interests include multiphase flow, CFD, and building environment.

Chang Hyun Sohn received his M.Sc. (Eng) in Mechanical Engineering in 1985 from KAIST. He also received his Ph.D. in Mechanical Engineering in 1991 from KAIST. He is a Professor of Mechanical Engineering, Kyungpook National University, since 1994. His research interests include CFD, PIV, flow-induced vibration, and thermal-hydraulics in the mechanical engineering field.